*ICLASS 2009, 11th Triennial International Annual Conference on Liquid Atomization and Spray Systems, Vail, Colorado USA, July 2009*

# GDI Multi-Hole Injector: Particle Size and Velocity Distribution for Single and Jet-to-Jet Evolution Analysis

L. Allocca*, S. Alfuso, L. Marchitto, G. Valentino
Istituto Motori, CNR
Via Marconi, 8 - 80125 Napoli, ITALY

**Abstract**

In this study, the spray from a multi-hole GDI injector has been characterized applying the Imaging and the Phase Doppler Anemometry techniques. A multi-holes injector, with a hollow-ellipsoid footprint structure, has been used. The spray pattern evolution has been analyzed injecting commercial gasoline at different injection pressures (10, 15 and 20 MPa). Pictures of the spray sequence have been captured, injecting the fuel in an optically accessible vessel at quiescent air conditions, ambient temperature and atmospheric backpressure, at different instant from the start of injection. The spray has been illuminated by high intensity flashes, synchronized with the injection system, that have allowed to capture the emerging fuel by a CCD camera, 1370 x 1048 pixels, 0.5 μs shutter time. The images have been processed by Image ProPlus software for extracting the main parameters of the spray evolution.
Local characteristics of the spray have been investigated along the jet axis by the phase Doppler anemometry in order to provide the size and two components of the droplets velocity: the axial and the radial ones. Data have been analyzed using the ensemble averaging technique in order to provide mean values. Additionally, the Weber number has been evaluated in order to provide further details of the atomization process.

## Introduction

The direct injection of gasoline (GDI) in SI engines makes these propulsors very attractive for fuel economy and performance improvements. The control of the injection process and the combustion chamber geometry enable this systems working in multi-mode operation: homogeneous charge for high load conditions, injecting the fuel during the intake phase, and stratified charge for part-low load conditions with fuel delivered during the compression stroke. GDI philosophy allows the combustion to proceed stably for a wide interval of global air-fuel ratios, namely stoichiometric and lean conditions. In this structure the characteristics of the fuel distribution inside the combustion chamber become determinant particularly at stratified charge where stoichiometric conditions in spark plug proximity are determinant to avoid misfiring phenomena [1-3].

The hollow-cone spray technology, from high pressure swirled injectors, has been applied up to last years, where the fuel was distributed widely in the combustion chamber due to the swirling motion. More recently, a multi-hole approach for the injector nozzle has been followed orienting the jets in the physical area where the fuel is required for the best air-fuel mixing [4,5,6]. The fragmentation of the delivered fuel in particles is an essential condition for their fast evaporation and mixing with the air during the ignition delay. An improvement of this process is given by the high injection pressure that in these fuelling systems may reach values up to 20 MPa.

In this paper, an experimental activity on the fuel dispersion from a GDI six-hole nozzle is reported, both in terms of tip penetration-cone angle and droplet size and velocity distribution. Image processing and phase Doppler anemometry techniques have been used for the global and local characterization of the fuel dispersion. The droplet atomization has been analyzed for different injection pressures and locations downstream the spray in a quiescent vessel. Analysis of size and droplets velocity as well the Weber number has been estimated along the injection time.

## Experimental apparatus

An injection apparatus, making use of an hydro-pneumatic pump activated by pressured gas, has been used for spraying gasoline through a six hole GDI injector. Input gas pressure ranging from 0.07 MPa to 0.7 MPa produced a linear output pressure of the fuel from 2.5 to 25 MPa. A reservoir pressure tank of 1.0 $dm^3$, located between the injection pump exit and the electroinjector, absorbed the pressure oscillations due to the needle opening and the air recharge. A piezoresistive pressure transducer, located on the pump-reservoir pipeline connection, allowed monitoring the pressure oscillations just before the injector connection. The injector has been housed in a pressure holder for connecting the pump to the accumulator. It has been driven by a Programmable Electronic Control Unit (PECU) able to operate in multinjection strategy mode with the needle opening time set trough the energizing current duration. Measurements of the fuel injection rate for the adopted strategies have been carried out by an AVL Meter operating on the Bosch principle to estimate the injected amount of fuel at different $P_{inj}$ [7,8].

*Corresponding author

The characterization of the fuel distribution has been made processing the images of the jets evolving in a high-pressure optically-accessible quiescent vessel at different backpressures. Commercial gasoline ($\rho$=740 kg/m$^3$) has been injected in a single pulse strategy at the pressures of 10, 15 and 20 MPa. The pulse durations have been calibrated for delivering 20 and 50 mg/str for all the pressures. The spray images have been collected at different instants from the start of injection by a synchronized high-resolution (1376x1040 pixels, 12 bit, 0.5 µs shutter time) CCD camera-enlightening flashes system. A wet seal spherical holder enabled the tilting of the injector on an angular range of +/- 15°, with respect to its axis, to control the spray orientation in the measurement vessel. This has permitted the alignment of the direction of the jet under examination perpendicularly to the optical axis of the CCD. The image of the jets, captured by the CCD camera, has been collected both in parallel (set-up A) and orthogonal (set-up B) conditions with respect to the spray propagation. A set of 5 images has been captured for each injection condition for a statistical analysis and cycle-to-cycle dispersion. Then, they have been handled off-line by processing software for measuring the parameters of the spray. Further details of the setup are reported in [9].

Velocity and droplet size measurements have been accomplished at ambient temperature and atmospheric pressure by the Phase Doppler Anemometry (PDA) technique. Simultaneous droplets size as well axial and radial components of the droplets velocity have been carried out at locations along a jet axis. The PDA system included an argon-ion laser operating at 514.5 and 488 nm, a 310 mm focal length transmitting optics with a beam separation of 65.0 mm and modular collecting optics working in forward scattering mode at an off-axis of 30°. A single aperture of 0.025 mm has been set into the receiver to limit the scattered light to the detectors. The transmitter and collecting optics have been mounted on an x-y-z translation stage that has allowed the positioning of the probe volume within the spray at different locations. A pulse generator has been used to trigger the PECU of the injection system and the PDA processor. The system allowed the reconstruction of size and velocity data along the injection timing with a time resolution of 20 µs. A sketch of the experimental apparatus is reported in figure 1.

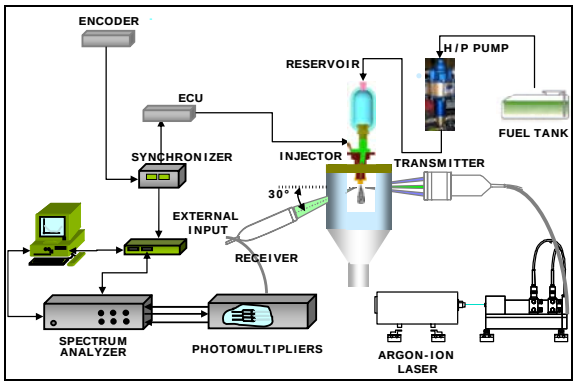


Figure 1 - PDA test bench

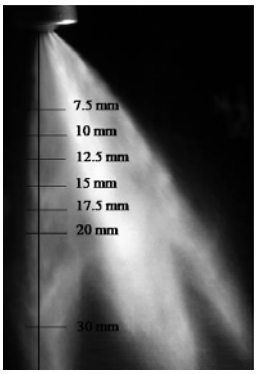


Figure 2 – Measurement grid

Experiments have been taken, at ambient temperature and atmospheric backpressure, injecting the fuel within a vessel under quiescent conditions with the bottom of the vessel connected to an exhaust blower to extract, under a low velocity co-flow air, fuel droplets. Experiments have been performed running the injection system at the frequency of 1 Hz, acquiring data over 300 injection cycles in order to build a data sample to get a reliable statistical analysis. The cycle-resolved data have been analyzed off-line by applying the ensemble averaging technique in order to estimate the axial and radial mean velocity and the average mean diameter (D10). Measurements have been performed on a single jet, out of the six ones, less interfering with the others. Test points have been located on the vertical axis of the jet, as shown in figure 2, which depicts the layout of the measurement grid. The investigated points have been 7.5, 10, 12.5, 15, 17.5, 20 and 30 mm from the nozzle.

**Results and Discussion**

The behaviour of the injected fuel, in terms of tip penetration and cone angle, has been analyzed to characterize droplets dispersion at the fixed conditions. The main hypothesis is that, at early time from the start of injection, all the jets behave in an independent way, thus the measurements have been made on a single jet. This condition could not be true for time greater than 1.0 ms where the jets swelling produce a no negligible interaction each other with influences both on droplets penetration and sizing. The processing analysis of the images has been carried out by a professional software taking into account background subtraction, filtering and edges determination for tip penetration and cone angle estimation. Further details on the adopted procedure can be found in [9].

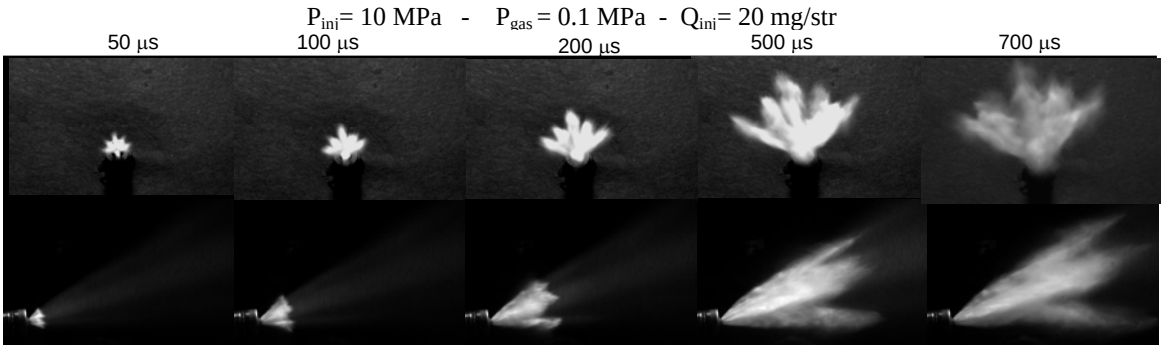


Figure 3 – Image sequences of the spray evolution for the A and B set-up at the indicated injection conditions

Images of the jets have been collected both in parallel and orthogonal conditions with respect to the spray propagation in the measurement vessel. Figure 3 reports a sequence of the images at 10 MPa injection pressure and atmospheric backpressure being 20 mg/str the fuel delivered. The propagation of the jets is clear and indicates the fuel distribution inside the vessel. The regular and non-interactive behaviour of the jets is up to 500 μs. Later the interference between them appears evident and the single evolution cannot be followed longer. Here, the spray has to be considered as a single, large and composite body. The lateral view of the spray evolution (set-up B) allows distinguishing the origin of the single jets close to the nozzle exit. Four single, well confined arrows appear in the CCD view plane while the last two are covered because in the back side. The capability to confine one jet in non-interactive condition with respect to the other enables to follow its penetration for long time, greater than 2.0 ms.

The effects of the injection pressure on the fuel penetration and cone angle, with 50 mg/str of injected fuel and atmospheric backpressure conditions, are reported in figure 4. Both profiles show a similar trend with a quite linear behaviour of the penetrations up to 500 μs. At later time, a logarithmic-bend in the shape is observed. Higher is the injection pressure longer penetration it produces. In fact, at 500 μs from the SOI, penetration values of 62.38 mm are reached for 20 MPa injection pressure curve respect to 54.94 mm for the 10 MPa. At 2000 μs, penetration values are 97.81 and 87.77 mm, respectively. The spray-cone angle curves show slightly lower asymptotic values for higher injection pressure condition. These values are 11.9° for 20.0 MPa and 12.4° for 10.0 MPa, respectively.

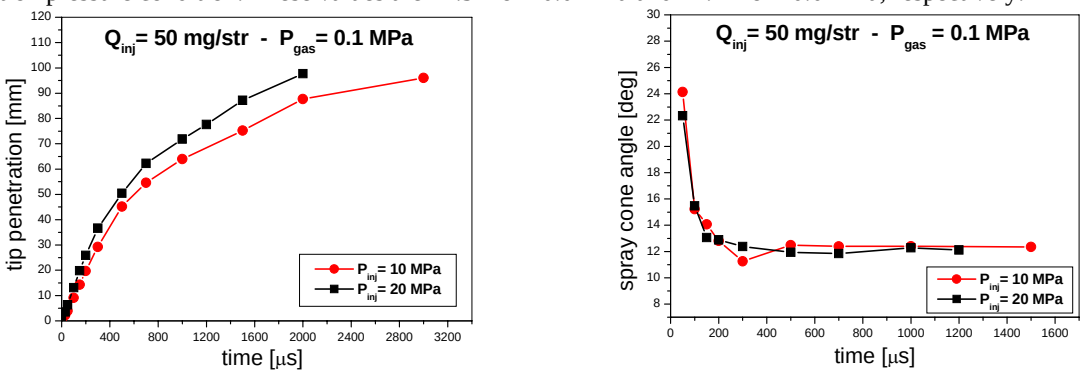


Figure 4 - Spray tip penetration and cone angle at 20.0 and 10. MPa injection pressures

**Velocity and droplets size.** Time-resolved size and velocity of droplets in the spray have been acquired by the PDA technique using the ensemble averaging procedure over 300 injection cycles, to estimate the mean diameter (D10) and two components of droplets velocity: axial and radial ones. Droplets distribution represents a great concern to provide reliable spray parameters, therefore some thousands of single droplets have been acquired for each data set, in order to estimate the axial and radial mean velocity, as well the mean diameter (D10). Measurements have been made, injecting the same amount of fuel (20 mg/str) at three injection pressures (10, 15, 20 MPa), on the jet that is non-interfering with the others as already pointed out in the experimental set-up paragraph.

In figure 5, the profiles of axial (top plot) and radial (middle plot) components of droplets velocity and droplets size (bottom plot), along the injection time at the injection pressure at 10 and 20 MPa, are reported. At 10 MPa (left figure), the first appearance of droplets, at 7.5 mm from the nozzle, is delayed by 0.5 ms that includes the dynamic delay of the injection system to deliver the first cluster of droplets plus the droplets flight time to reach the sampling volume. As a general trend, the axial and radial components profiles are almost the same at any investigated loca-

tion. Looking at the axial velocity profiles, they show an early decreasing trend during the transient needle opening stage (500-760 µs for the location at 7.5 mm from the nozzle) with a development to a constant and regular trend during the steady state part of injection. In fact, first droplets, injected in stagnant conditions, fast give up their momentum to the air and decelerate. Then, next droplets coming from the nozzle are injected into the entrained air motion and thus not slow down as fast as the earlier ones, penetrating farther downstream. This behaviour is well depicted by looking at the profiles of axial velocity components with the initial decreasing trend replaced by a rise.

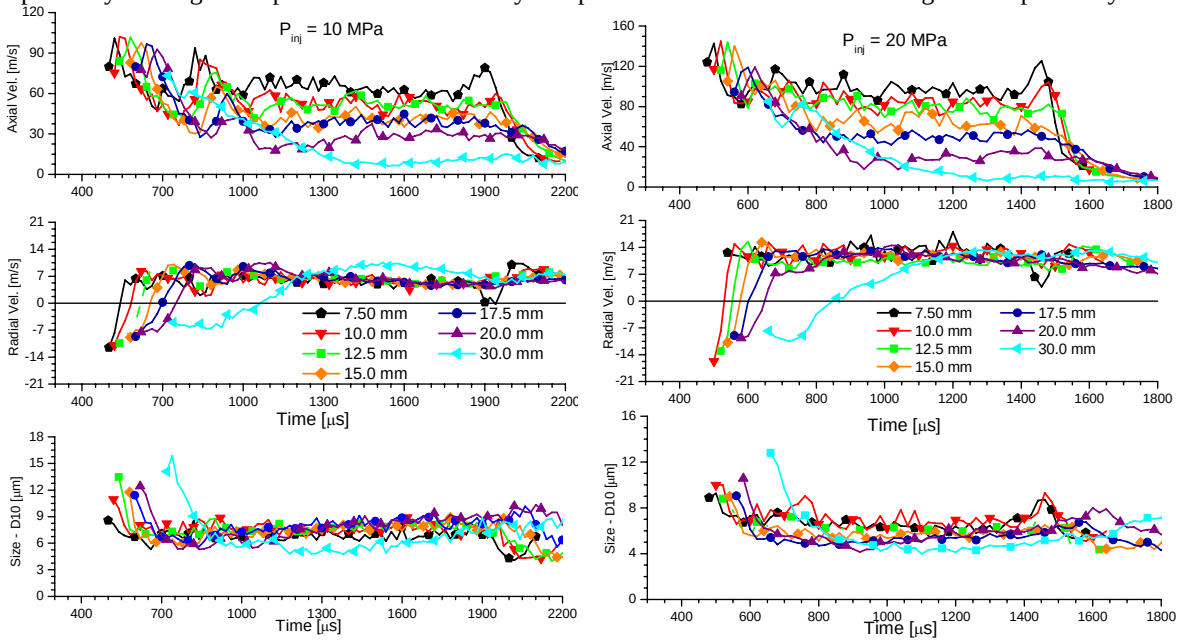


Figure 5 –Droplets size, axial and radial components of droplets velocity at 10 MPa (left plot.) and 20 MPa (right plot.)

The location at 30 mm from the nozzle, which represents the leading edge of the spray, shows droplets that are less decelerated by aerodynamic forces being characterized by smaller droplets formed later during the injection process. The axial component of droplets velocity exhibits, during the steady interval of injection, an intensity scaling moving from the near to the far field of the jet with values ranging from about 70 m/s to 10 m/s at 7.5 mm and 30 mm from the nozzle, respectively. The spray near to the nozzle (up to 10 mm) yields droplets attaining the highest values in the axial velocity during the steady state period of injection, with a final rise found at the end of injection. The increase of axial velocity at the end of injection may be due to the transient process of the needle closure that makes the nozzle deliver bigger droplets travelling at higher velocity.

Looking at the radial component of the droplets velocity, it can be observed an inward direction because of the air entrainment during the transient stage of injection. It is followed by a fast reverse motion that set the radial component to a constant value of about 7 m/s along the steady state period. An exception may be distinguished in the common behaviour of the radial profiles. In fact, the location at 30 mm from the nozzle starts from an inward direction but, its trend has a slower slope than the former positions. Further, during the steady state period, the intensity of the radial component shows higher values thus denoting a different fluid-dynamic behaviour of the spray edge.

As illustrated in the experimental arrangement, the spray characteristics have been also investigated to give the droplets size and show the effect of the injection pressure. The plot at the bottom of figure 5 illustrates the mean diameter (D10) profiles of droplets generated by the nozzle at the injection pressure of 10 MPa. It may be observed an unambiguous decreasing trend of droplets size during the early stage of injection with values ranging from 8.5 to about 16 µm, moving away from the nozzle. It is worth mentioning that the droplet size distribution highlights a large scattering with an average rms of about 10 µm. The size plot shows that the first detection of droplets is time shifted moving away from the nozzle, due to the flight time of droplets to reach the sampling point. During the steady state period of injection, the spray is formed by droplets having almost overlapping values of the mean diameters that range from 6.5 to 9 µm. The location at 30 mm from the nozzle exhibits an exception displaying droplets size from 5 to 7 µm in diameter. The spray characteristics have been investigated also at the injection pressure of 20 MPa, injecting the same amount of fuel (20 mg/str). Results of the axial and radial components of droplets

velocity and size are illustrated in the right plots of figure 5. The general trend of the axial component profiles are very similar to those obtained at 10 MPa with increased values due to the higher injection pressure. The same assessment is displayed during the initial transient period and the following steady state interval, in which a scaling of the axial component intensity is obtained, moving away from the nozzle. The final stage of injection is marked by an increase of the axial component intensity, more evident with respect to the condition at 10 MPa. In fact, the locations at 7.5 and 10 mm from the nozzle depict a relevant rise in the axial component intensity that matches to the increase in the mean diameter, as it can be observed looking at the size plot. The radial component profiles also display similar trends to those at 10 MPa but show values almost twice (14 m/s). Size profiles, obtained at the injection pressure of 20 MPa, provide, during the steady interval of injection, values ranging from 5 to 7 µm, again with the exception of the location at 30 mm from the nozzle that achieves values of about 4.5 µm.

The spray characterization has been further investigated at an intermediate injection pressure of 15 MPa. Here in the paper, because similar profiles of axial and radial components of droplets velocity have been obtained, only the effect of the injection pressure on droplets size is discussed. Profiles of the mean diameter at the locations of 7.5 and 10 mm from the nozzle are reported in figure 6, both at 7.5 (left plot) and 10 mm (right plot) from the nozzle. The increase in the injection pressure makes the spray produce smaller droplets with analogous profiles. In fact, examining the plot, bigger droplets are produced during the early stage of injection with a tendency to a size reduction and a subsequent constant value during the steady state process.

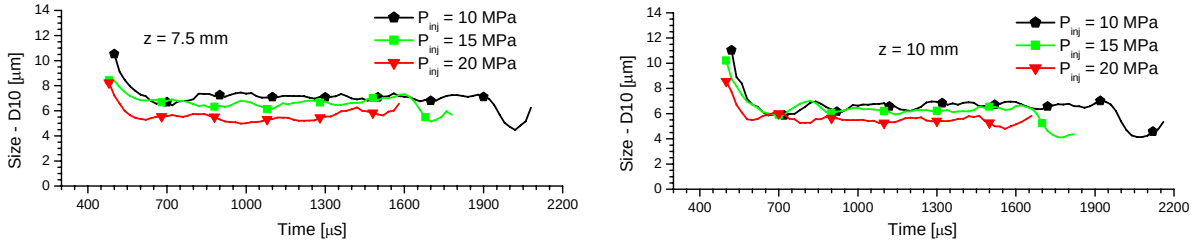


Figure 6 – Droplets size at different injection pressures for the locations at 7.5 and 10 mm from the nozzle

**Weber number** - Fuel atomization process involves a breakup mechanism that takes place for the first liquid cluster out of the nozzle as it encounters the undisturbed flow field or the stagnant conditions of the surroundings, like the present setup. The first clusters of droplets transfer their momentum to the air and fast slow down. The unsteady air motion induced by the momentum exchange with the droplets makes possible build up the air-flow entrainment supporting the breakup. The onset of droplet cracking due to aerodynamic forces is related to the Weber number defined as the ratio of the inertia force to the surface tension force and computed according to the equation:

$$We = \frac{\rho \cdot V_r^{\,2} d_p}{\sigma}$$

where $\underline{V_r}$ is the relative velocity of the ambient gas, $d_p$ is the droplet diameter, $\rho$ the gas density, $\sigma$ the surface tension. In this paper the small droplets lower than 5 µm were chosen as representative of the air flow motion whereas, the droplets velocity vector was computed considering the ensemble averaged resultant of axial and radial components. Figure 7 shows profiles of Weber number obtained at the injection pressure of 10 and 20 MPa.

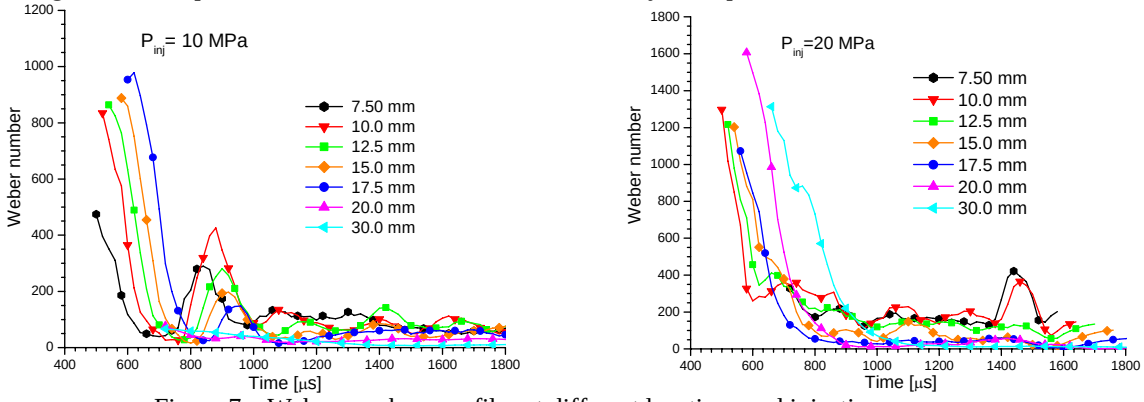


Figure 7 – Weber numbers profiles at different locations and injection pressures

It can be observed that, for both injection pressures, the droplets breakup is fast during the transient stage of injection because of the rapid rise in the injection pressure rate, decaying on a short time to a low value. Considering that for Weber numbers greater than about 12 ($We_{cr}$), a breakup is expected, the atomization process should go under a catastrophic type of breakup [10]. Looking at the plot illustrating the Weber numbers at 10 MPa, it can be observed secondary peaks, time phased to the locations away from the nozzle, having a decreasing intensity. Subsequent to this process, the Weber numbers of the locations from 7.5 to 17.5 mm have a tendency to get a steady trend with small fluctuations still higher than the $We_{cr}$. The locations at 20 and 30 mm from the nozzle seem not involved by a breakup process that on the contrary occurs for distances closer to the nozzle.

At the injection pressure of 20 MPa, the Weber numbers are indicative of a catastrophic type of breakup during the early stage of injection with decreasing trend that are not reaching low values as for the condition at 10 MPa. In fact, for the locations from 10 to 15 mm from the nozzle it seems that the secondary peaks are included in the fast falling shape. At later time, the same locations are still involved in a breakup process considering that the *We* decay to fluctuating values about 100-180. Locations at longer distances from the nozzle do not show at all the secondary peak, and reach *We* about 20-25 indicative of an unimportant breakup process. As a conclusive remark, it is interesting to report the behavior at the location 7.5 mm that does not show a fast decay and not attain high *We* numbers, fluctuating along the entire injection interval that may be indicative of a region close to the breakup length for the investigated nozzle.

**Conclusions**

The spray from a multi-hole GDI injector has been investigated applying the Imaging and the Phase Doppler Anemometry techniques. The investigation has been focused on the spatial and temporal behaviour of the jets, in terms of overall fuel distribution, penetration and cone angle, and local fluid-dynamic structure, like droplet size and velocities, that are important factors for validation of atomization and break-up sub-models. The main results may be summarized as it follows:

- The injection pressure affects the penetration but not the spray cone angle that rapidly decays to a steady value;
- The axial component of droplets velocity shows a decreasing trend followed by a steady value scaled with respect to the distance from the nozzle. The radial one gives an initial inward direction with a subsequent fast reverse motion to a constant value that is strongly affected by the injection pressure.
- The atomization process is affected by the injection pressure with the production of smaller droplets at higher pressures; during the early stage of injection bigger droplets are produced with a tendency to decay to constant values during the steady state interval of injection.
- In the early stage of injection, the jet undergoes to a catastrophic breakup attaining high *We* numbers both at 10 and 20 MPa. At the injection pressure of 20 MPa the breakup process is confined in a region up to 15 mm from the nozzle whereas longer distances are involved in a non-significant breakup.

**References**

1. Cathcart G., Railton D.,“Improving Robustness of Spray Guided Combustion Systems: The Air-Assisted Approach”, SAE Paper 2001-53-60, JSAE Spring Convention 2001.
2. Kume T., Iwamoto Y., Iida K., Muratami K., Akishino K., Ando H., Combustion Control Technologies for Direct Injection SI Engine, SAE Paper 960600, 1990.
3. Lake T.H., Stokes J., Whitaker P. A., Crump J. V., Comparison of Direct Injection Gasoline Combustion Systems. SAE Paper 980154, 1998.
4. Kawajiri K.T., Yonezawa H., Ohuchi H., Sumida M., Katashiba H.,“Study of Interaction Between Spray and Air Motion, and Spray Wall Impingement”, SAE Paper 2002-01-0836, 2002.
5. Landenfeld T., Kufferath A., Gerhard J., “Gasoline Direct Injection – SULEV Emission Concept”, 2004 SAE World Congress, Paper 2004-01-0041.
6. Alfuso, S. , Allocca, L., M. Greco, Montanaro, A., Valentino, G.,”Time and Space Characterization of Multihole GDI Sprays for IC Engines by Images Processing and PDA Techniques” ILASS 2008 Sept. 8-10, 2008,Italy
7. Bosch, W. , "The Fuel Rate Indicator: a New Measuring Instrument for Display of the Characteristics of Individual Injection", SAE Paper 6607496, 1966
8. Wallace, I., “ Injection Rate Gauge: Pass Off Information and User Instructions” - Fuel & Engine Management Systems, Graz - December 2002
9. Alfuso, S., Allocca, L., Caputo, G., Corcione, F.E., Montanaro, A., Valentino, G., “Experimental Investigation of a Spray from a Multi-jet Common Rail Injection System for Small Engines” SAE_NA 2005-24-9
10. Borman, G.L., Ragland, K.W., *Combustion Engineering*, WCB/McGraw-Hill, 1998